Available online at www.sciencedirect.com
ScienceDirect
Ceramics International 35 (2009) 3161–3168
CERAMICS INTERNATIONAL
www.elsevier.com/locate/ceramint

Preparation and characterization of porous hydroxyapatite through polymeric sponge method

Iis Sopyan [a,*], Jasminder Kaur [b]

[a] Department of Manufacturing and Materials Engineering, Faculty of Engineering, International Islamic University Malaysia, PO Box 10, Jalan Gombak, 50728 Kuala Lumpur, Malaysia
[b] Department of Materials Science and Engineering, Malaysia University of Science and Technology, Dataran Usahawan Kelana, Petaling Jaya, 47301 Selangor, Malaysia

Received 28 August 2008; received in revised form 4 February 2009; accepted 4 May 2009
Available online 6 June 2009

Abstract

Porous hydroxyapatite samples were prepared via polymeric sponge method using commercial hydroxyapatite (HA) powder. The effects of sintering rate, stirring time and HA concentration on porosity, compressive strength and crystallinity of the porous bodies were evaluated. The study found that a faster sintering rate resulted in higher apparent density, higher compressive strength and better crystallinity. A longer stirring time also yielded the same results. 42 wt.% HA concentration was found to be the optimal concentration to achieve higher compressive strength and crystallinity, and lower porosity. The compressive strength of the porous bodies varied from 1.8 to 10.5 MPa for a porosity gradient of 34.3–59.8%. The results showed that the compressive strength is strongly dependent on porosity. Mechanically, the HA porous bodies developed in the study can be accepted as bone implants as the average compressive strengths are well within that of cancellous bone.

Keywords: Porous hydroxyapatite; Bone implant; Polymeric sponge; Characterization

1. Introduction

In recent years, particular attention has been paid to the preparation of HA bioceramics with porous morphology. There is a vast application of porous HA in the biomedical engineering area. Porous HA have been applied for cell loading, drug-releasing agent, and the most extensively for hard tissue scaffolds [1]. In the highlight of bone implant applications, its development is addressed to mimic the micro- and macro-porous architecture of the mineral phase of living bone [1]. Bone tissue is hoped to grow well into the pores, increasing strength of the HA implant.

It was realized that dimension and morphology of pores are crucial factors for an excellent osteointegration [2]. Minimum pore size required to enable ingrowth of the surrounding bone together with blood supply, is about 100–150 μm for macropores [3], and even at pores of as small as 50 μm osteoconduction is still possible [4]. Some reports state that it should be 200–500 μm for colonization of osteoblast in the pores, fibrovascular ingrowth and finally the deposition of new bone [5]. Other important requirements for porous implants are interconnectivity of the pores for the penetration of the osteoblast-like cells inside the pores as well surface roughness for the attachment of cells.

There are a large number of methods to produce porous hydroxyapatite, including incorporation of volatile organic particles in HA powder [6], polymeric sponge method [7–11], gel casting of foams [12], starch consolidation [13], microwave processing [14], slip casting [15–17], and electrophoretic deposition technique [18]. The differences in the methods used to produce porous HA can directly affect the pore characteristics. Incorporating organic particles with ceramic powder results in a porous structure of closed, poorly interconnected, and non-uniform pores. Gel casting of foams can be applied to produce ceramic scaffolds with high mechanical strength. The disadvantage of this technique is that it typically results in a structure of poorly interconnected pores, and non-uniform pore size distribution. The starch consolidation method is based on the swelling ability of starch when it is heated to 80 °C in the presence of water. This method can result in flexural strengths

* Corresponding author. Tel.: +60 320564592; fax: +60 320564477.
E-mail address: sopyan@iiu.edu.my (I. Sopyan).

0272-8842/$36.00
doi:10.1016/j.ceramint.2009.05.012

of as low as 2 MPa for pore volume fractions of 70% and as high as 15 MPa for pore volume fractions of 45%. The microwave processing technique has produced porous HA with a porosity of up to 73%. The porosity of the ceramic can be controlled by varying the morphology of the starting materials, adjusting green density, as well as altering the sintering time and temperature. The slip casting method can be used to fabricate porous HA bodies with porosity of larger than 50% and pore sizes of up to 750 μm. Also, the pore size distribution of the porous bodies can be controlled by determining the sintering temperature. Eletrophoretic deposition (EPD) of submicron HA powders produces uniform and crack-free bulk porous HA scaffolds with good mechanical strength and interconnected porosity with a wide range of pore sizes.

The most common method for fabricating open-cell (reticulate) porous ceramics is by replication of a porous polymer substrate. Porous ceramics obtained from reticulated polymer substrates have a number of distinct properties such as controllable pore size and complex ceramic shapes for different applications [7]. The polymeric sponge method is performed by impregnating porous cellulosic substrates with HA slurry. Porous HA prepared by the polymeric sponge method has shown to have a controllable pore size and interconnected pores but poor mechanical strength for load bearing applications. Literature has shown that the polymeric sponge method results in a proper pore size distribution, as osteoconduction requires. This is characterized by the existence of micro/meso/macropores with adequate degree of interconnection [9,19].

We have reported our results on the development of porous hydroxyapatite using polymeric sponge method [1,8]. The samples which were prepared using sol–gel method-derived HA powders showed a considerable compressive strength. Preliminary results shown that its good pore connectivity and surface roughness accelerated the fast growth of VERO cell proliferated using the porous bodies as the microcarries [1]. In this paper, we want to present the effect of sintering rate, stirring time and HA concentration on porosity, compressive strength, and crystallinity of porous hydroxyapatite prepared.

2. Experimental

2.1. Materials

For the preparation of porous HA samples, hydroxyapatite, distilled water, a dispersing agent and cellulosic sponges were used. The hydroxyapatite powders were purchased from Merck KGaA, Germany, while the dispersing agent (Duramax D3005) was purchased from Rohm and Haas, Philadelphia, PA. Cellulosic sponge was purchased from Spontex SpA, Italy.

2.2. Preparation of porous HA

By using the commercial HA powder, slurries were prepared with an adjusted loading of HA, using Duramax of D-3005 type as dispersant. Commercial cellulosic sponges were used which are able to recover to its original shape after impregnation and is fully eliminated at a temperature of about 600 °C. Cellulosic sponges were cut into circular samples of 1 cm diameter. HA suspensions were prepared by dissolving HA powder into distillated water. The powder was put into distillated water little by little in stirring condition to assure the dissolving homogeneity. Then, the dispersant was added to the solution in various compositions. Three dispersant compositions have been applied to HA suspensions as shown in Table 1. After soaking into the slurry, the sponges were dried in ambient air and then subjected to heat treatment at 600 °C for 1 h to eliminate organic matrix. Sintering was conducted at 1200 °C for 1 h. The sintering rate was varied to compare the effects of slow and fast sintering rates on the porosity, compressive strength and crystallinity of porous bodies. The dimension and mass of all samples were measured before and after heat treatment.

Table 1
Preparation condition of porous hydroxyapatite.[a]

Sample	Water (g)	HA concentration (wt.%)	Stirring time (h)	Sintering rate
S1	15.7	44	20	25 °C/min
S2	15.7	44	20	220 °C/h
S3	16.7	42	20	220 °C/h
S4	16.7	42	4	220 °C/h
S5	20.0	38	20	220 °C/h
S6	20.0	38	4	220 °C/h

[a] The amounts of added HA and dispersing agent were adjusted at 12.6 and 0.4 g, respectively.

2.3. Characterization of HA powder and porous samples

The crystallinity and structure of the HA powder and the sintered porous samples were analyzed by XRD. The XRD spectra were collected by means of a Shimadzu Diffractometer XRD-6000, using Cu K_α radiation at 30 mA, 40 kV. Scans were performed between 2θ values of 10° and 80° at a rate of $2^\circ\ min^{-1}$. The porosity of all samples was determined by calculating its apparent and relative densities. Compression test is used to characterize porous HA samples. The compressive strength of porous HA was measured using Lloyd LR10K plus mechanical tester. The compressive load was applied at a crosshead speed of 0.4 mm min^{-1} on the cylindrical samples until failure. The compressive strength was calculated from the maximum load registered during the test divided by the original cross section area. Morphological evaluation on the HA powder and porous bodies have been done using a JEOL JSM 6700F field emission scanning electron microscope (FESEM), equipped with energy dispersive spectrometry (EDS) microprobe analyzer. The samples were mounted on conducting carbon tape, vapor coated with palladium using JEOL JFC 1600 AutoFine Coater, and were visualized using an accelerating voltage of 5 keV.

3. Results and discussion

Characterization on the commercial HA powder used in the study has been reported elsewhere but here it can be

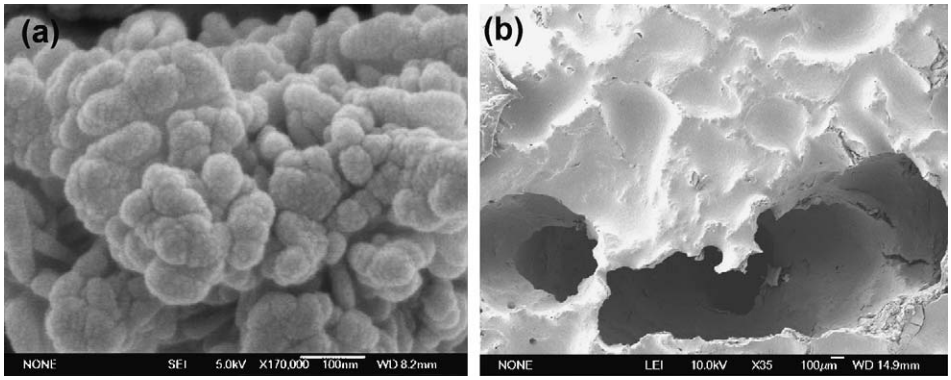

Fig. 1. SEM images of HA powder (a) and porous HA (b).

summarized that its morphology consists of nanometric primary particle agglomerated into micrometric aggregates, with very fine individual particles of 75–150 nm average diameter. From EDS and XRD analysis, the Ca/P ratio for the HA powder was calculated to be 1.66, thus showing that the purity of the HA powder was almost 100% [8]. Its FESEM picture is presented in Fig. 1(a). The hydroxyapatite porous bodies resulted after sintering process show good pore connectivity as shown in Fig. 1(b). Interconnectivity of the pores is needed for the penetration of the osteoblast-like cells inside the pores and subsequent attachment onto the pore walls. Variation in pore density was found in some samples due to insufficient suspension stability during the drying process. There are macropores which exist in the body with 100–500 μm diameter. The tunnels link the macropores outside to the pores within the porous body.

The effects of three parameters, sintering rate, stirring time and HA concentration, were evaluated on porosity, compressive strength and crystallinity of the porous bodies. To evaluate the first parameter, sintering rate, samples S1 and S2 were compared. The HA concentration and stirring time were kept constant while sintering rate was varied (as indicated in Table 1). The apparent densities and porosities were determined using methods described elsewhere [8]. As seen in Fig. 2, sample S1 was found to have higher average apparent density, compressive strength and Young's modulus, whereas the average porosity was lower. The average compressive strength for sample S1 was 10 MPa for an average apparent density of 2.03 g/cm^3 and average porosity of 35.9% (Table 2). In this study, it was observed that a faster sintering rate resulted in a higher apparent density and thus, higher compressive strength. Higher sintering rate likely resulted in more favorable densification of amorphous structure, leading to higher density and thus better mechanical strength. The findings obtained in this study are in agreement with a study by Gibson and Ashby, who reported a proportional correlation between apparent density and mechanical strength [20]. Fig. 3 shows the compression test result of one of the porous bodies of sample S1. All samples displayed a linear-elastic region followed by a collapse until rupture.

The effect of crystallinity was evaluated by XRD. The XRD patterns of porous HA shown in Fig. 4 are in good agreement with those of standard HA (JCPDC #9-432) as well as the results obtained by Ramay and Zhang [21] and Kwon et al. [24]. The XRD results of the porous samples did not show the presence of secondary phases confirming that the sintering process did not disrupt the HA phase. However, the degree of crystallinity of the two porous bodies could not be concluded from XRD spectra as the peak intensity of the two samples were not significantly different as seen is Fig. 4. FESEM images in Fig. 5 shows that sample S1 has a much larger crystal size and higher degree of fusion between the individual crystals indicating higher crystallinity. The higher porosity of sample S2 is clearly seen in the FESEM micrograph in Fig. 5(b). The sample has open microporosity on the macropore walls ranging from 0.2 to 1 μm. This also establishes that sample S2 has a lower density compared to sample S1 as calculated earlier. This result concludes the results found in XRD. Sample S1 was heat

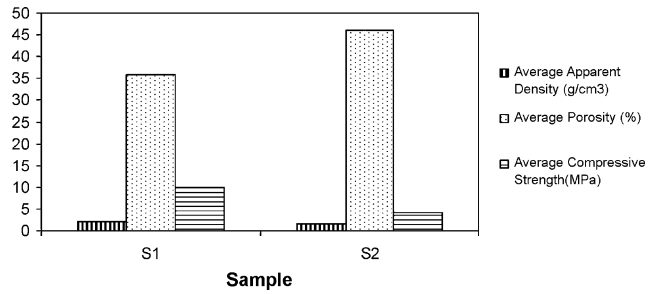

Fig. 2. Average apparent density, compressive strength and porosity of samples S1 and S2.

Table 2
Porous HA preparation conditions and physical properties of porous samples S1, S2, S3, S4, S5 and S6.

Sample	Average apparent density (g/cm^3)	Average porosity (%)	Average compressive strength (MPa)	Average Young's modulus (MPa)
S1	2.03	35.9	10.0	655
S2	1.69	46.2	4.3	275
S3	2.08	34.3	10.5	579
S4	1.81	42.7	6.4	385
S5	1.60	49.4	3.2	215
S6	1.27	59.8	1.8	61

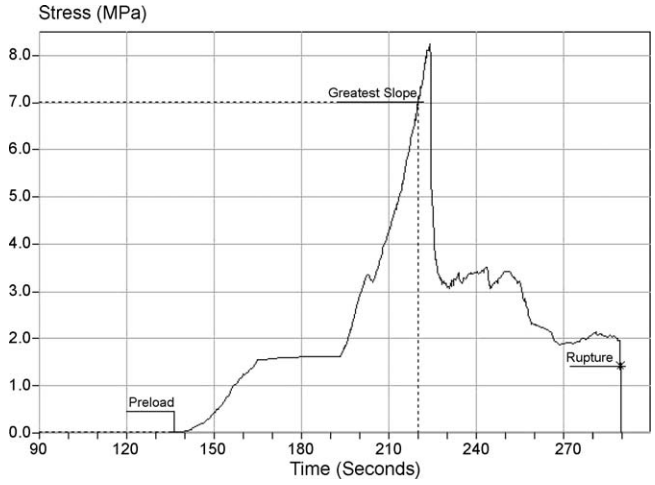

Fig. 3. Compression test result of one of the porous bodies of sample S1.

treated at a much faster rate compared to sample S2, and thus, the heating is more progressive leading to a higher compressive strength, crystallinity, as well as lower porosity.

The effect of stirring time was assessed by comparing samples S3 and S4 as well as samples S5 and S6. The porous HA preparation conditions can be found in Table 1 whereas the physical properties are listed in Table 2. All specimens broke in a manner similar to elastic–brittle foam, with a load peak followed by a collapse until rupture region. Fig. 6 shows the comparison of samples S3, S4, S5, and S6 for their average apparent density, compressive strength, and porosity. As can be seen from the comparison of samples S3 and S4, an increase in stirring time increased the compressive strength and apparent density but decreased porosity. The same observation can be made for samples S5 and S6. Increasing the stirring time results in the breakdown of agglomerates and the slurry obtained tends to be more homogeneous. This in turn reduces the porosity of the porous bodies, and increases compressive strength and apparent density as well as crystallinity.

For the increased apparent density from 1.27 to 2.08 g/cm^3, the compressive strength increased from 1.8 to 10.5 MPa. This is higher than the 0.55–5 MPa compressive strength obtained for the apparent densities of 0.0397–0.783 g/cm^3, as reported by Ramay and Zhang [21]. Hing et al. on the other hand, reported that they succeeded in preparing porous HA with compressive stress of 1–11 MPa for the increased apparent density from 0.38 to 1.25 g/cm^3 [22]. With respect to total porosity, the value of 10.5 MPa average compressive strength for a specimen with 34.3% average porosity is still low when compared to the 16.1 MPa reported by Guicciardi et al. [23] for the specimen of 56% total porosity.

The XRD spectra of the porous samples indicate that the sintering process did not alter the composition of HA in the porous bodies. Comparing the XRD spectra of samples S3 and S4, it can be seen that the degree of crystallinity increased with stirring time, as shown in Fig. 7. This result was further confirmed by comparing the peaks intensity of samples S5 and S6 (Fig. 8). Fig. 9 shows the FESEM pictures of samples S3, S4, S5 and S6. It is evident from the lower number of voids seen in Fig. 9(a) that sample S3, with longer stirring time, has lower porosity and higher density than sample S4 (Fig. 9(b)). The larger crystal size and fewer boundaries between particles with more unified

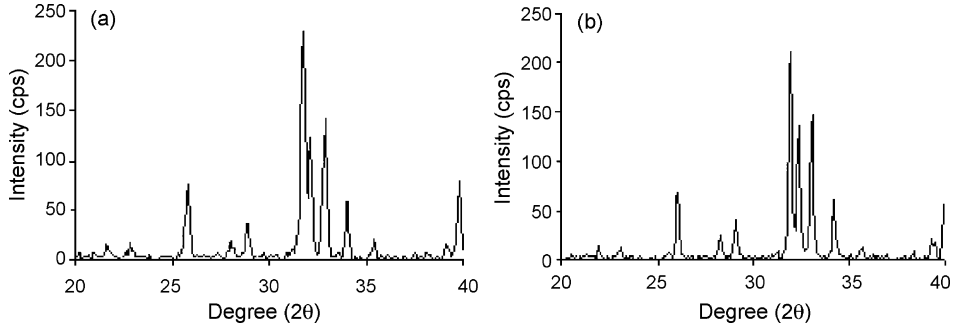

Fig. 4. XRD patterns of porous samples (a) S1 and (b) S2.

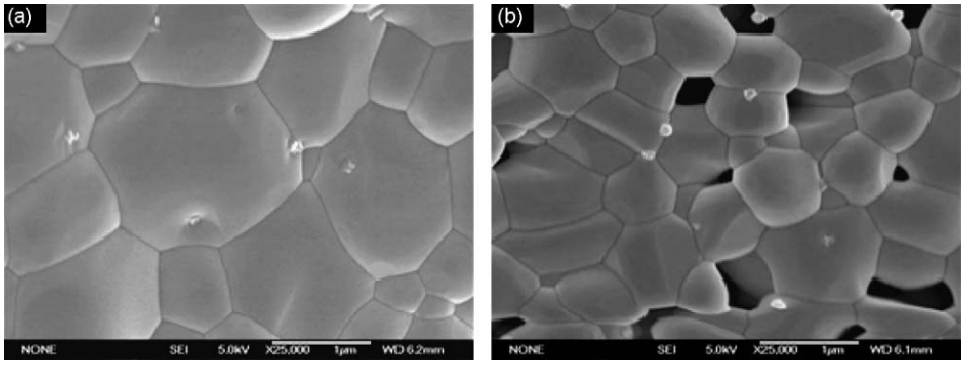

Fig. 5. FESEM images showing the microporosity of samples (a) S1 and (b) S2.

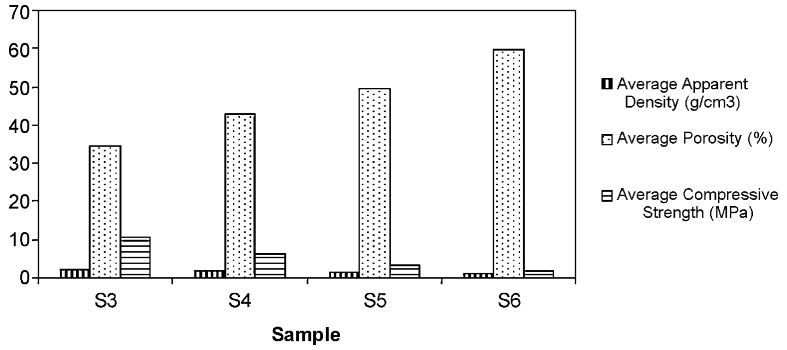

Fig. 6. Average apparent density, compressive strength and porosity of samples S3, S4, S5 and S6.

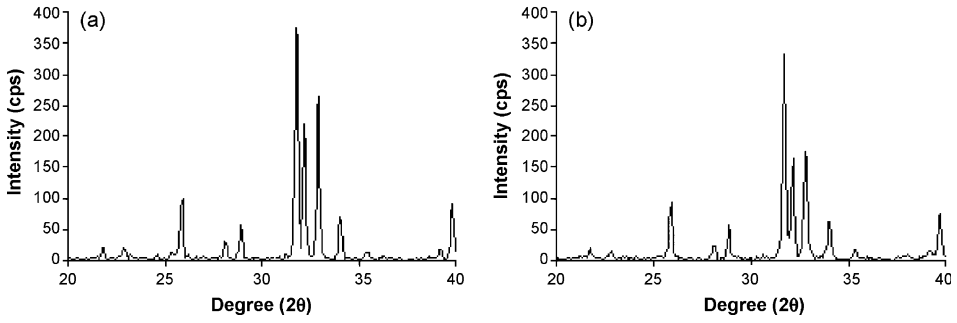

Fig. 7. XRD patterns of porous samples (a) S3 and (b) S4.

particles seen in S3 indicate higher crystallinity. The same results were acquired by comparing FESEM micrographs of samples S5 and S6, as illustrated in Fig. 9(c) and (d). This was in good agreement with the XRD results discussed earlier. Increasing the stirring time produced more homogenous slurry and thus, increased the crystallinity of the porous structure.

In order to obtain higher densities and better mechanical properties for porous bodies, a high ceramic concentration in the prepared slurry is required. On the other hand, if the HA concentration is too high; the slurry would have a high viscosity, leading to difficulty in impregnating the cellulosic sponges as slurry penetration into the pores becomes difficult. This will in turn produce highly porous materials after heat treatment [21]. Similarly, if the HA concentration is too low, the number of pores-penetrating HA particles will be less, resulting in lower mechanical strength. Therefore, 44 and 38 wt.% HA concentrations were selected as the highest and lowest concentrations, respectively. Porosity varies with the suspension composition, and higher porosity tends to give lower compressive strength. Although high porosity is favored as the high surface area/volume ratio promotes more progressive cell adhesion to the scaffold and thus encourages bone tissue regeneration, its mechanical properties are poor. It was well known that compressive strengths of porous human cancellous bones vary between 2 and 12 MPa (See for example Literature 1). Although bone ingrowth lead to the enhanced compressive strength of porous implants; where for high porosity implants this observation is more obvious due to faster bone growth, an optimum balance between porosity and strength must be achieved in the as-prepared implants to assure that the implant can withstand the applied forces in the course of operation and in the initial stage at the implantation site.

To evaluate the effect of HA concentration on porosity, compressive strength and crystallinity, samples S2, S3 and S5

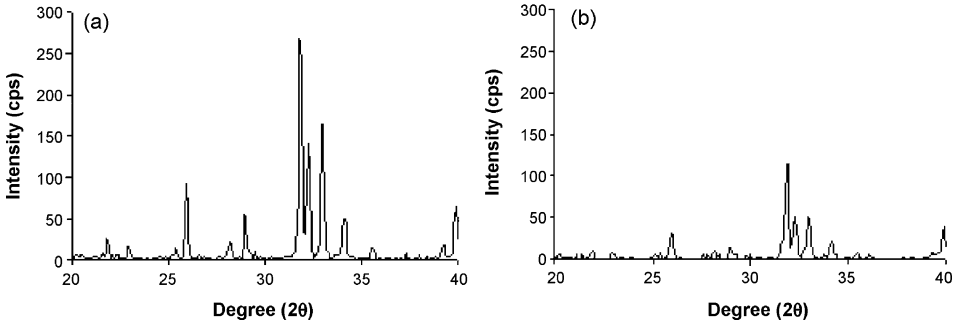

Fig. 8. XRD patterns of porous samples (a) S5 and (b) S6.

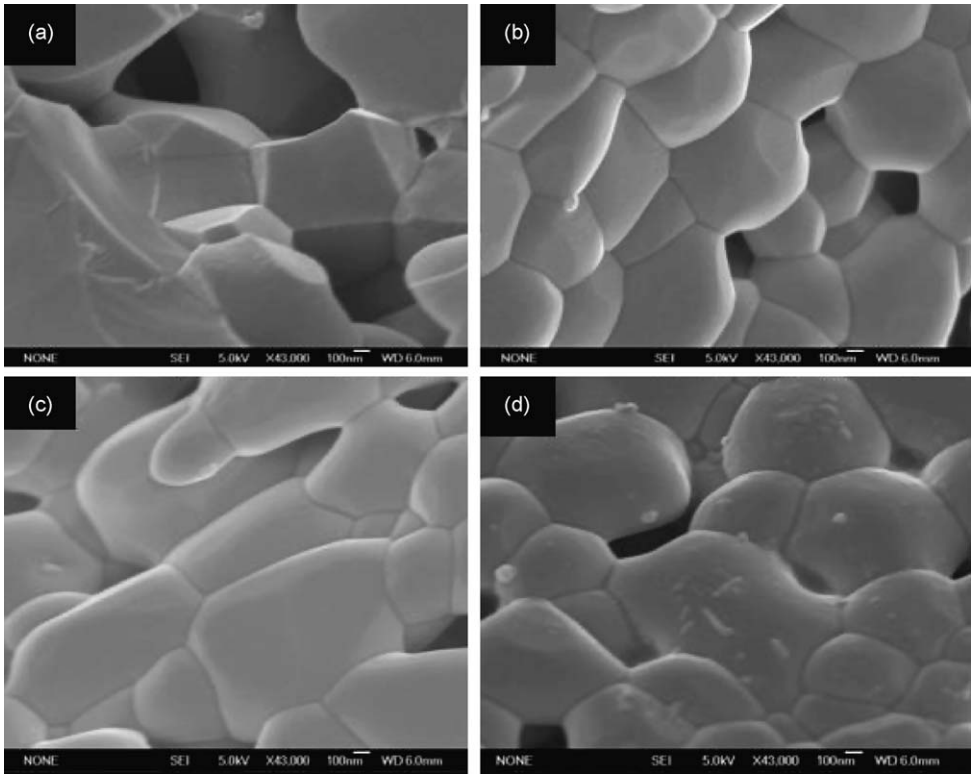

Fig. 9. FESEM micrographs of samples (a) S3, (b) S4, (c) S5 and (d) S6.

with HA concentrations of 44, 42 and 38 wt.%, respectively, were compared. From the FESEM images in Fig. 10, it can be seen that as the HA concentration was increased from 38 to 42 wt.%, the pores became more interconnected with more dense and thicker pore walls, indicating higher density. This finding was in agreement with that reported by Ramay and Zhang [21]. The results in Table 2 indicate that sample S3 with a HA concentration of 42 wt.% has the highest apparent density (2.08 g/cm^3) and compressive strength (10.5 MPa), but the lowest porosity (34.3%). The relationship between average porosity and average compressive strength is presented in Fig. 11. The average compressive strength increased from 3.2 MPa at 49.4% porosity to 10.5 MPa at 34.3% porosity when the HA concentration was increased from 38 to 42 wt.%, but reduced to 4.3 MPa at 46.2% porosity when HA concentration was further increased to 44 wt.%. This indicates that HA concentration significantly affects the mechanical properties of porous HA and an optimal HA concentration is needed to obtain porous bodies with acceptable mechanical strength while showing good porosity. A compromise between HA loading and slurry fluidity should be achieved for successful impregnation. In fact, large cavities were found in the center of some high HA loading samples most probably as the result of incomplete slurry penetration into the pores. Considering that our porous HA still show acceptable compressive strength for human spongy bone implants while showing considerable porosity (for examples S5, and even S6 which still shows 1.8 MPa compressive strength at a porosity as high as 60%) the simplified sponge method we employed in this work is appropriate to produce porous HA for human cancellous bone implants.

The XRD patterns shown in Fig. 12 are in good agreement with the corresponding values of standard HA (JCPDS #9-432). As can be seen from the peak intensity in the XRD spectra, sample S3 with 42 wt.% HA loading shows the highest crystallinity, followed by samples S2 and S5, consecutively. This trend is proportional with respective compressive strength. We therefore presume that homogeneity of the slurry plays

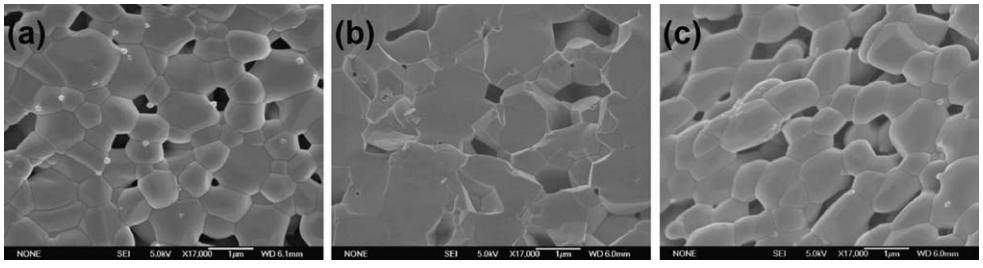

Fig. 10. FESEM micrographs of samples (a) S2 (44 wt.%), (b) S3 (42 wt.%) and (c) S5 (38 wt.%).

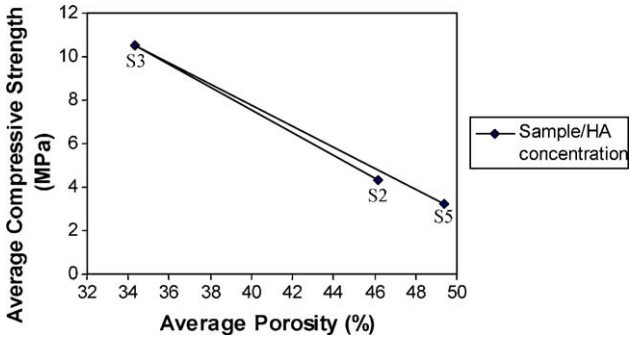

Fig. 11. Average porosity and average compressive strengths of samples S2, S3 and S5.

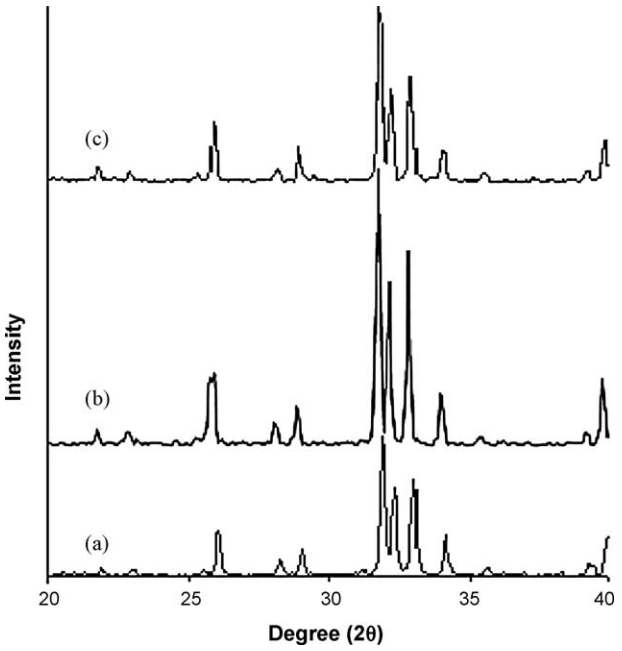

Fig. 12. XRD patterns of porous samples (a) S2, (b) S3 and (c) S5.

important role in this mechanism. The concentration of 42 wt.% likely produced more stable and homogeneous slurry, allowing complete penetration of HA particles into the pores. Enough particles in the pores resulted in even, progressive particles fusion when subjected to sintering. Such particles fusion behavior is difficult to happen in samples S2 and S5. Sample S5 with 38 wt.% HA concentration presumably has homogeneous and stable slurry, but less HA particles in the pores limit it from good particles fusion upon sintering, on the other hand, the slurry of sample S2 (44 wt.% HA loading) was likely not stable enough to avoid precipitation after impregnation course, leading to uneven distribution of HA particles in the pores. Its higher viscosity also caused more difficult penetration of HA particles, which in turn gave higher porosity. Micropore morphology shown by SEM images in Fig. 10 confirmed the findings. It can be deduced, therefore, that the HA concentration of 42 wt.% is the optimal concentration to achieve higher density and better mechanical properties for porous HA bodies.

4. Conclusions

Porous HA bodies with various porosities and compressive strengths were successfully produced via the polymeric sponge method using commercial hydroxyapatite powder as the starting material. Sintering of the slurry-impregnated polymeric sponges did not alter the HA composition for all samples. All porous samples contained micropores of 0.2–1 μm and macropores of 100–500 μm in diameter. The effects of processing parameters like sintering rate, stirring time and HA concentration on the physical properties were studied. The average compressive strength of the porous bodies varied between 1.8 and 10.5 MPa for a decrease in porosity from 59.8% to 34.3%; concluding that compressive strength is inversely dependent on porosity. It was established that the higher compressive strength was also attributed to higher apparent density and crystallinity. Faster sintering rate resulted in higher apparent density, higher compressive strength and better crystallinity due to more progressive heating. Stirring slurry for a prolonged period of time also resulted in higher compressive strength due to its better homogeneity. An optimum HA concentration is critical in order to obtain high porosity porous bodies but with acceptable compressive strength for human spongy bone implant application. In this case, it was found that all the prepared porous samples are mechanically in the range of human cancellous bone; where S3 with 42 wt.% HA loading was considered as the best sample as it shows the highest compressive strength of 10.5 MPa at 34.3% porosity.

Acknowledgements

The authors are grateful to the financial supports available from IIUM Research Center through a research grant LT37. The authors gratefully acknowledge Brs. Syamsul Kamal Arifin and Danial Mohammed by some experimental works.

References

[1] I. Sopyan, M. Mel, S. Ramesh, K.A. Khalid, Porous hydroxyapatite for artificial bone applications, Science and Technology of Advanced Materials 8 (2007) 116–123.
[2] J.C. Le Huec, T. Schaeverbeke, D. Clement, J. Faber, A. Le Rebeller, Influence of porosity on the mechanical resistance of hydroxyapatite ceramics under compressive stress, Biomaterials 16 (1995) 113–118.
[3] S.F. Hulbert, S.J. Morisson, J.J. Klawitter, Tissue reaction to three ceramics of porous and non-porous structures, Journal of Biomedical Materials Research 6 (1972) 347–374.
[4] B.S. Chang, C.K. Lee, K.S. Hong, H.J. Youn, H.S. Ryu, S.S. Chung, K.W. Park, Osteoconduction at porous hydroxyapatite with various pore configurations, Biomaterials 21 (2000) 1291–1298.
[5] T.J. Flatley, K.L. Lynch, M. Benson, Tissue response to implants of calcium phosphate ceramics in the rabbit spine, Clinical Orthopedic 179 (1983) 246–252.
[6] L.L. Hench, J. Wilson, An Introduction to Bioceramics, World Scientific Publishing Co. Ltd., 1993.
[7] J. Tian, J. Tian, Preparation of porous hydroxyapatite, Journal of Materials Science 36 (2001) 3061–3066.

[8] I. Sopyan, J. Kaur, R. Singh, Hydroxyapatite porous bodies via polymeric sponge method using commercial powder, in: Proceedings of Conference on Advanced Materials, 2005, pp. 505–513.
[9] B. Palazzo, M.C. Sidoti, N. Roveri, A. Tampieri, M. Sandri, L. Bertolazzi, Controlled drug delivery from porous hydroxyapatite grafts: an experimental and theoretical approach, Materials Science and Engineering C 25 (2005) 207–213.
[10] M. Fabbri, G.C. Celotti, A. Ravaglioli, Hydroxyapatite-based porous aggregates: physico-chemical nature, structure, texture and architecture, Biomaterials 16 (1995) 225–228.
[11] A. Tampieri, G. Celotti, S. Sprio, C. Mingazzini, Characteristics of synthetic hydroxyapatites and attempts to improve their thermal stability, Materials Chemistry and Physics 64 (2000) 54–61.
[12] P. Sepulveda, J.G. Binner, S.O. Rogero, O.Z. Higa, J.C. Bressiani, Production of porous hydroxyapatite by gel-casting of foams and cytotoxic evaluation, Journal of Biomedical Materials Research 50 (2000) 27–34.
[13] L.M. Rodríguez-Lorenzo, M. Vallet-Regi, J.M.F. Ferreira, Fabrication of porous hydroxyapatite bodies by a new direct consolidation method: starch consolidation, Journal of Biomedical Materials Research 60 (2002) 232–240.
[14] Y. Fang, D.K. Agarwal, D.M. Roy, R. Roy, Fabrication of porous hydroxyapatite ceramics by microwave processing, Journal of Materials Research 7 (1991) 490.
[15] L.M. Rodríguez-Lorenzo, J.M.F. Ferreira, Development of porous ceramic bodies for applications in tissue engineering and drug delivery systems, Materials Research Bulletin 39 (2004) 83–91.
[16] G. Carutenuto, G. Spagnuolo, L. Ambrosio, L. Nicolais, Macroporous hydroxyapatite as alloplastic material for dental applications, Journal of Materials Science: Materials in Medicine 10 (10/11) (1999) 671–676.
[17] M. Rusnah, M. Andanastuti, B. Idris, The influence of sintering temperature on the porosity and strength of porous hydroxyapatite ceramics, The Medical Journal of Malaysia 59 (Suppl. B) (2004) 158–159.
[18] J. Ma, C. Wang, K.W. Peng, Electrophoretic deposition of porous hydroxyapatite scaffold, Biomaterials 24 (2003) 3505–3510.
[19] A. Tampieri, G. Celotti, S. Sprio, A. Delcogliano, S. Franzese, Porosity-graded hydroxyapatite ceramics to replace natural bone, Biomaterials 22 (2001) 1365–1370.
[20] L.J. Gibson, M.F. Ashby, Cellular Solids: Structure and Properties, Cambridge Solid State Science Series, second ed., Cambridge University Press, 1997.
[21] H.R. Ramay, M. Zhang, Preparation of porous hydroxyapatite scaffolds by combination of the gel-casting and polymer sponge methods, Biomaterials 24 (2003) 3292–3302.
[22] K.A. Hing, S.M. Best, W. Bonfield, Characterization of porous hydroxyapatite, Journal of Materials Science: Materials in Medicine 10 (1999) 135–145.
[23] S. Guicciardi, C. Galassi, E. Landi, A. Tampieri, Rheological characteristics of slurry controlling the microstructure and the compressive strength behaviour of biomimetic hydroxyapatite, Journal of Materials Research 16 (2001) 163–170.
[24] S.H. Kwon, Y.K. Jun, S.H. Hong, I.S. Lee, H.E. Kim, Calcium phosphate bioceramics with various porosities and dissolution rates, Journal of American Ceramic Society 85 (2002) 3129–3131.